# THE CHOICE OF TRACKING FEATURES IN ULTRASOUND-BASED STRAIN IMAGING ANALYSIS

*Weichuan Yu and James S. Duncan*

Image Processing and Analysis Group, Yale University
BML 332, 310 Cedar Street, New Haven, CT 06520-8042

## ABSTRACT

In order to quantify the left ventricular (LV) strain variation from echocardiographic data, the use of the underlying radio frequency (RF) signal is sometimes proposed to provide higher estimation precision than the B-scan signal. In this paper, we argue that this approach is appropriate only when the deformation between two successive frames is very small. In the analysis of large deformation (such as cardiac deformation), the advantage of using RF signal disappears. Simulation and phantom studies show that the B-scan signal is more robust to frame-to-frame decorrelation than the RF signal when the correlation coefficient of the corresponding RF signal is lower than a threshold value, which is typically equal to $0.985$.

## 1. INTRODUCTION

Echocardiography is widely used at patients' bedside in the emergency room and intensive care units in the hospital to provide real-time data for the diagnosis of heart disease. It is very desired to derive quantitative strain variation of the left ventricle (LV) from echocardiographic images since such quantitative information is proven to be a sensitive index in the diagnosis [1]. This, however, is a challenging task due to the high noise level and feature variation in echocardiographic images. Previous shape-based approach [2] used LV boundary shape information to address this problem with some success. But it still requires tedious segmentation step of the LV boundary surface. Moreover, it provides no information about the mid-wall region of the myocardium, which is critical to distinguish transmural injury from non-transmural injury.

Our motivation is to estimate mid-wall motion directly from echocardiographic images. Towards this end, we are interested in using the concept of texture feature tracking. This idea has been identified as speckle tracking (e.g.[3]), which uses the unique speckle patterns (i.e. the results of constructive or destructive interference of different back-scattering waves [4]) as tracking feature. Currently, the most commonly used features in echographic images are RF signal [5, 6] and B-scan signal [7, 8], although the pass-band energy was also used [9]. While the success in [5, 10] suggests that the RF signal is the first choice in deformation analysis under high precision requirement as it provides finer structure than the B-scan signal, it is unclear if this is still true if we have large deformation such as the LV deformation, where the *motion-feature decorrelation* (i.e. the motion parameters estimated from feature based speckle tracking fail to represent the underlying tissue motion) becomes the major source of estimation error for **all** feature-based pointwise tracking.

Although the problem of decorrelation has been addressed from different points of views (e.g. [11, 12, 5]), no study is given regarding which is the best tracking feature for large deformation analysis. Our contributions in this paper are: 1. We propose that the tracking metric for pointwise strain estimation should be chosen based on a feature-related reliability measure and we show that the correlation coefficient is such a quantitative measure. 2. We show with simulations and phantom examples that the B-scan signal is more favored as tracking feature than the RF signal in the analysis of large deformation.

The rest of the paper is organized as follows: In Section 2, we review the difference between the RF signal and the B-scan signal and describe the influence of this difference on the displacement estimation. In Section 3, we validate our statement with simulations and phantom examples. This paper is concluded with some discussions in section 4.

## 2. COMPARING THE RF SIGNAL WITH THE B-SCAN SIGNAL

The echocardiographic imaging process can be approximated as a linear convolution between a point spread function (PSF) $H(\vec{X})$ and a set of tissue scatterers $T_n(\vec{X};\vec{X}_n)$. The PSF in the far field of the transducer is assumed to be a 3-D Gaussian enveloped cosine function [8]

$$H(\vec{X}) = e^{-\frac{1}{2}\vec{X}^T\Gamma\vec{X}} \cdot \cos(2\pi\vec{X}^T\vec{U}_0). \qquad (1)$$

Here $\vec{X} = (x, y, z)^T$ denotes the spatial coordinates with positive $z$ pointing to the wave propagation direction, $\vec{U}_0 =$

$(0, 0, u_{z0})^T$ denotes the spatial frequency of the ultrasound wave, and $\Gamma$ is a $3 \times 3$ diagonal matrix whose diagonal elements read $\frac{1}{\sigma_x^2}$, $\frac{1}{\sigma_y^2}$, and $\frac{1}{\sigma_z^2}$, respectively. The variances of the Gaussian $\sigma_x$, $\sigma_y$, and $\sigma_z$ are not necessarily the same. We set the location of the transducer at $(0, 0, 0)$ in the 3-D spatial space. The tissue scatterer is assumed to be very small so that it can be represented as a Dirac function [8]

$$T_n(\vec{X}; \vec{X}_n) = a_n \delta(\vec{X} - \vec{X}_n), \tag{2}$$

where $a_n (0 < a_n < 1)$ represents the echogenicity of the scatterer and $\vec{X}_n = (x_n, y_n, z_n)^T$ denotes the center of randomly distributed scatterer. During the imaging process, the tissue region can be decomposed into a discrete set of resolution cells. In each resolution cell, the convolution between the PSF and tissue scatterers yields the RF signal

$$\begin{aligned} RF(\vec{X}; \vec{X}_n) &= \sum_{n=1}^{N} T_n(\vec{X}) * H(\vec{X}; \vec{X}_n) \\ &= A(\vec{X}; \vec{X}_n) cos(\phi(\vec{X}; \vec{X}_n)). \end{aligned} \tag{3}$$

In a commercial echocardiography system, an RF image is usually converted into a B-scan image before displaying on the screen. Ideally, this process can be described as converting the RF signal into an *analytical signal* and then extracting the magnitude of the analytical signal, yielding

$$I_B(\vec{X}; \vec{X}_n) = |A(\vec{X}; \vec{X}_n)|. \tag{4}$$

Eqs. (3) and (4) are to show that the RF signal can be decomposed into an amplitude part and a phase part, while the B-scan signal only keeps the amplitude part. It should be noticed that both $RF$ and $I_B$ are functions of $\vec{X}$ **and** $\vec{X}_n$. Actually, this dependence on $\vec{X}_n$ is the reason of decorrelation since deformation changes the relative positions of different $\vec{X}_n$s and thus changes the result of interference. Strictly speaking, the variation of $\vec{X}_n$s will also cause the variation of $a_n$s and $N$s in resolution cells, making the decorrelation even more unpredictable. Mathematically, decorrelation compensation is an ill-posed inverse problem because there are more unknown parameters (such as $\vec{X}_n$) than the data available (e.g. intensity values). This problem can be ignored only if the decorrelation is small enough, where we can approximately assume that the feature variation caused by decorrelation is caused by noise.

In the domain of small deformation analysis, some approaches (e.g. [6, 10]) have shown that the RF signal provides higher tracking precision than the B-scan signal since the RF signal preserves the phase information. In the spatial domain, the phase information is embedded into the carrier function which is a cosine wave. As the spatial frequency of the carrier function (i.e. $u_{z0}$) is much higher than that of the B-scan signal, the phase information provides a finer sub-structure inside the envelope signal (i.e. $I_B$). If there is no deformation or deformation is very small, this sub-structure is stable and thus the decorrelation is negligible. Then the RF signal provides higher tracking precision than the B-scan signal. If the deformation is large enough, however, the mis-alignment of both the envelope signal and the sub-structure is inevitable. Under the same amount of deformation, the impact of mis-alignment is much larger on the subtle sub-structure than on the envelope signal due to the high spatial frequency $u_{z0}$ in the carrier function of the RF signal. Consequently, the decorrelation of the RF signal is severer than that of the B-scan signal.

The meaning of "negligible decorrelation" and "severe decorrelation" is elusive in above description. We need a quantitative criterion to clearly distinguish these two situations. Remembering that correlation coefficient has been used as a similarity measure, we can also use it as a quantitative index of decorrelation. In the next section, we will quantitatively compare the performance of RF signal and of B-scan signal in deformation analysis and show that the B-scan signal is more appropriate in the analysis of large deformation.

## 3. EXPERIMENT

We start the comparison with a simulation example so that the ground truth is easily available. We use Eq. (3) to simulate an RF image volume and use Eq. (4) to convert the RF volume into its B-scan version. Then, we change the positions of $\vec{X}_n$s to simulate deformation. The parameters used in the simulation are listed in table 1. We construct a cube with the size of $10 \times 10 \times 5$ mm. We assume the resolution cell size of the transducer is $1 \times 1 \times 0.5$ mm. Thus, the cube totally contains 1000 resolution cells. Supposing the speckles in these resolution cells are fully developed, we produce 10000 uniformly distributed random variables to simulate the positions of scatterers, whose echogenicity coefficients $a_n (n = 1, \cdots, 10000)$ obey the normal distribution between 0 and 1.

| Parameter | Value |
|---|---|
| transducer frequency $f_0$ | 4 MHz |
| sound speed in tissue $c$ | 1540 m/s |
| wavelength $\lambda$ | 0.385 mm |
| spatial frequency of sound $u_{z0}$ | 5.195 cycles/mm |
| resolution cell size $\Delta X \times \Delta Y \times \Delta Z$ | $1 \times 1 \times 0.5$ mm |
| standard deviation along the x-axis $\sigma_x$ | 0.426 mm |
| standard deviation along the y-axis $\sigma_y$ | 0.426 mm |
| standard deviation along the z-axis $\sigma_z$ | 0.213 mm |
| x-axis range [ $X_{min}, X_{max}$ ] | $[-5, 5]$ mm |
| y-axis range [ $Y_{min}, Y_{max}$ ] | $[-5, 5]$ mm |
| z-axis range [ $Z_{min}, Z_{max}$ ] | $[0, 5]$ mm |
| sampling interval ( $\delta x, \delta y, \delta z$ ) | $(\frac{1}{8}, \frac{1}{8}, \frac{1}{16})$ mm |

**Table 1**. The parameters in the simulation.

We use a correlation-based algorithm for motion tracking. In Fig. 1, we plot the variation of mean correlation coefficients of different features with respect to the deformation parameter. As part of comparison, we show the mean values of the estimation error with the corresponding variance values drawn as vertical lines on top of the bars. The comparison shows that the B-scan signal has higher correlation coefficients and less estimation error than the RF signal when the deformation parameter is larger than or equal to $0.3\%$.

The correlation coefficients of the RF signal have mean values of $0.989$ and $0.976$ when the deformation parameters are equal to $0.2\%$ and $0.3\%$, respectively. Interestingly, the correlation value of $0.985$ (just between the above two values) was used in [13] as a threshold value to guarantee reliable tracking. This coincidence suggests that the value around $0.985$ is typically the threshold of correlation coefficient below which the RF signal would not have better performance than the B-scan signal.

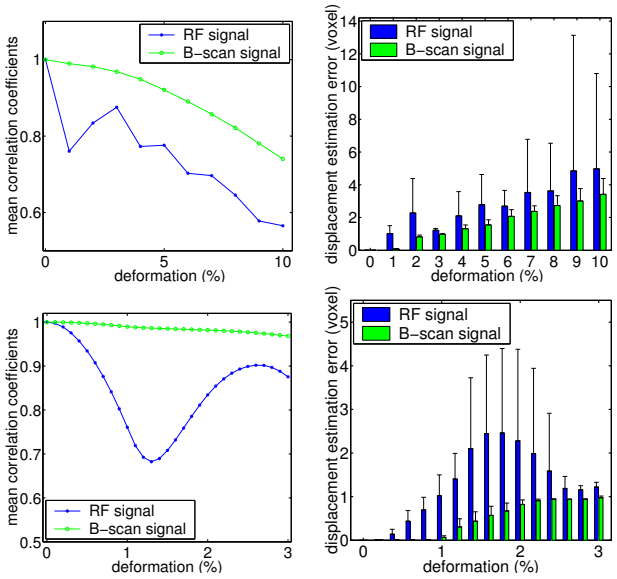


**Fig. 1**. **Row 1 Left:** Mean correlation coefficients of different features in the case of deformation (with the unit of percentage in volume height). The zig-zag structure in the RF signal based plot is caused by periodic property of phase signal. See text for details. **Row 1 Right:** Mean values of the displacement estimation error with the corresponding variance drawn as vertical lines on top of the bars. **Row 2:** Enlarged plots of counterparts in Row 1 with the deformation only between zero and three percents.

The zig-zag structure in the RF signal-based coefficient plot is caused by the fact that the carrier of the RF signal is a periodic function and the phase difference is always modulated by $\pi$. The phase difference will start to decrease after reaching its maximum of $\pi$. The enlarged plot in row 2 of Fig. 1 shows this variation clearly. Interestingly, this periodicity sometimes helps to improve the estimation precision.

Fig. 2 shows an phantom example with large deformation. The soft gelatin phantom contains a stiff cylindrical inclusion and a soft, thin, fluid-filled channel. To produce external compression, the top surface of the phantom was compressed downward with the transducer by $5\%$ of the volume height. Each resolution cell is discretized by roughly eight samples. The relative stiffness difference in three different parts can be seen in the strain image reconstructed from the displacement field. For such a large compression, a direct application of correlation-based tracking algorithm would fail since the signal coherence is severely broken down. Fortunately, the scaling change and the translational motion of the compressor are known (or can be easily derived from images). Thus, we can apply the so-called *global companding* technique (cf. [5] for details) to restore the coherence of signals to some extent without varying the *pure* decorrelation. To make a fair comparison, we apply the same global companding with the same parameters to both features. Fig. 2 shows the correlation coefficients of different features after the global companding. These correlation coefficient images are also called trashograms in [10]. The B-scan signal has a higher mean value of correlation coefficients than the RF signal. Correspondingly, the strain image using the B-scan signal is still smooth, while the smoothness of the strain image using the RF signal breaks down. This example along with the simulation example clearly shows that the B-scan signal is more robust to large deformation than the RF signal.

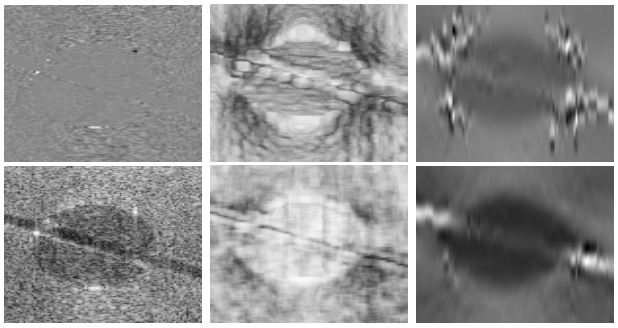

**Fig. 2**. **Row 1: Left:** RF signal of the phantom image; **Middle:** Correlation coefficients of the RF signal after a $5\%$ compression. We use a $101 \times 11$ window to estimate the correlation coefficients after applying the global companding technique [5]. The mean value equals $0.608$. The border region is not considered in the estimation. **Right:** Strain images reconstructed from the displacement field. The smoothness of the strain values in the gelatin region breaks down. **Row 2:** Counterpart of row 1 using the B-scan signal with the mean value of correlation coefficients equal to $0.708$.

## 4. DISCUSSION

The RF signal has a finer structure than the B-scan signal. Thus, it is of advantage to use the RF signal in the analysis of small deformation. But the RF signal is also more vulnerable to deformation due to its finer structure. We make this statement clear by showing that there exists a threshold in the correlation coefficient below which the B-scan signal provides more robust results than the RF signal. This comparison has implications in cardiac motion analysis: The relative LV strain variation between systole and diastole can reach up to $30\%$. The highest frame-rate of the newest 3-D echocardiography transducer is currently no more than $20$ Hz. Thus, an average strain variation between $1.5\%$ and $2.0\%$ is expected in the deformation analysis between neighboring frames. According to our simulation analysis, the B-scan signal still can be used in the pointwise motion tracking framework, while the RF signal is useful **only** when the extremely high frame rate becomes available.

This conclusion is based on a quantitative reliability measure — the correlation coefficient. The nice point about this measure is that it does not depend on a specific feature. Also, it can be calculated directly from images even without knowing the motion parameters.

In the comparison, we use a simple correlation-based approach. The estimation precision is limited by the resolution available. Applying the phase sensitive method jointly (e.g. [13]) may further improve the precision of the RF signal-based estimation, providing that the estimation error in the initial estimation (which is usually obtained using the B-scan signal) is not beyond the capture range of the phase sensitive method (which is typically $\lambda/2$ with $\lambda$ denoting the spatial wavelength of the acoustic wave). Otherwise, the aliasing effect may appear. We do not enter the details here due to the space limitation.

In the future work, we would like to get access to the RF signal of the new 3-D echocardiography transducer and continue the evaluation with more realistic examples of LV deformation.

## 5. ACKNOWLEDGMENT

We thank M. Insana and C. Barakat from University of California, Davis for their valuable discussions and for providing the phantom data.

## 6. REFERENCES

[1] P. Shi, A.J. Sinusas, R.T. Constable, E. Ritman, and J.S. Duncan, "Point-tracked quantitative analysis of left ventricular surface motion from 3-D image sequences," *IEEE Trans. Medical Imaging*, vol. 19(1), pp. 36–50, 2000.

[2] X. Papademetris, A.J. Sinusas, D.P. Dione, and J.S. Duncan, "Estimation of 3D left ventricular deformation from echocardiography," *Medical Image Analysis*, vol. 5(1), pp. 17–28, 2001.

[3] L.N. Bohs, B.J. Geiman, M.E. Anderson, S.C. Gebhart, and G.E. Trahey, "Speckle tracking for multi-dimensional flow estimation," *Ultrasonics*, vol. 38, pp. 369–375, 2000.

[4] R.F. Wagner, S.W. Smith, J.M. Sandrik, and H. Lopez, "Statistics of speckle in ultrasound B-scans," *IEEE Trans. Sonics and Ultrasonics*, vol. 30(3), pp. 156–163, 1983.

[5] P. Chaturvedi, M.F. Insana, and T.J. Hall, "2-D companding for noise reduction in strain imaging," *IEEE Trans. UFFC*, vol. 45(1), pp. 179–191, 1998.

[6] M.A. Lubinski, S.Y. Emelianov, and M. O'Donnell, "Speckle tracking methods for ultrasonic elasticity imaging using short-time correlation," *IEEE Trans. UFFC*, vol. 46(1), pp. 82–96, 1999.

[7] J. Meunier and M. Bertrand, "Ultrasonic texture motion analysis: Theory and simulation," *IEEE Trans. Medical Imaging*, vol. 14(2), pp. 293–300, 1995.

[8] J. Meunier, "Tissue motion assessment from 3d echographic speckle tracking," *Physics in Medicine and Biology*, vol. 43, pp. 1241–1254, 1998.

[9] F. Yeung, S.F. Levinson, D. Fu, and K.J. Parker, "Feature-adaptive motion tracking of ultrasound image sequences using a deformable mesh," *IEEE Trans. Medical Imaging*, vol. 17(6), pp. 945–956, 1998.

[10] M.A. Lubinski, S.Y. Emelianov, and M. O'Donnell, "Adaptive strain estimation using retrospective processing," *IEEE Trans. UFFC*, vol. 46(1), pp. 97–107, 1999.

[11] J. Meunier and M. Bertrand, "Echographic image mean gray level changes with tissue dynamics: A system-based model study," *IEEE Trans. Biomedical Engineering*, vol. 42(4), pp. 403–410, 1995.

[12] R.L. Maurice and M. Bertrand, "Lagrangian speckle model and tissue-motion estimation — theory," *IEEE Trans. Medical Imaging*, vol. 18(7), pp. 593–603, 1999.

[13] K. Kaluzynski, X. Chen, S.Y. Emelianov, A.R. Skovoroda, and M. O'Donnell, "Strain rate imaging using two-dimensional speckle tracking," *IEEE Trans. UFFC*, vol. 48(4), pp. 1111–1123, 2001.